

# Investigating A *Clean* Natural Gas-based Hydrogen Production Process for Electricity Generation in Power Plants

Shervan Babamohammadi, William George Davies, Salman Masoudi Soltani

Department of Chemical Engineering, Brunel University London, Uxbridge UB8 3PH, United Kingdom  
[Shervan.babamohammadi@brunel.ac.uk](mailto:Shervan.babamohammadi@brunel.ac.uk) [William.davies@brunel.ac.uk](mailto:William.davies@brunel.ac.uk) [Salman.masoudisoltani@brunel.ac.uk](mailto:Salman.masoudisoltani@brunel.ac.uk)

**Abstract**—This study investigates a clean hydrogen production process (based on a CH<sub>4</sub> feedstock flow rate of 1000 kmol/h) integrated with an onsite hydrogen-combustion power plant. A rate-based kinetic model is used to develop steam methane reforming (SMR) and water gas shift (WGS) reactions in the reformer. The impact of auto thermal reforming (ATR) on hydrogen purity and the generated power is investigated by analyzing the correlation between temperature, pressure, and steam-to-methane ratio. A full factorial design matrix is used to investigate the potential interactions among the operational variables with a set of key performance indicators (KPIs) i.e. hydrogen purity and generated power. The ATR leads to higher hydrogen purity and generated power at lower feed temperatures. Also, increasing the steam-to-methane ratio leads to increased hydrogen purity and generated power in both scenarios. Pressure is found to play a critical role in power generation but has a less pronounced effect on hydrogen purity in comparison. Employment of ATR has been found to be beneficial to achieve higher hydrogen purity and increased power generated at lower feed temperatures, while simultaneously minimizing CO<sub>2</sub> emissions.

**Keywords** — clean hydrogen, zero-emission, power plant, hydrogen-combustion, hydrogen turbine, CO<sub>2</sub> capture.

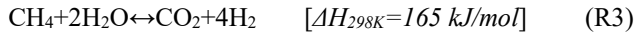
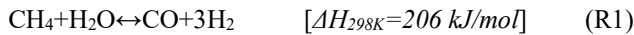
## I. INTRODUCTION

National Centres for Environmental Information reported that the Earth's surface temperature increased by 0.08°C per decade since 1880, marking 2021 as the sixth hottest year globally. According to several scenarios presented by Intergovernmental Panel on Climate Change (IPCC), by 2100, the global temperature can be 1.4–4.4 °C higher than it was before the *industrial revolution*, causing sea level rise, flooding, ocean acidification, and extinction of crops and species [1, 2]. Carbon dioxide (CO<sub>2</sub>) is the main contributor to climate change with the major share associated with the energy sector, chemical industries, transportation, and cement manufacturing [3]. The power sector is committed to reducing CO<sub>2</sub> emissions and upgrading current technologies to produce clean and low-carbon electric power [4].

Hydrogen (H<sub>2</sub>) is an essential part of the transition to a green economy, with the Global Hydrogen Review in 2021 reporting an increase of 50% demand since 2000 [5]. This includes 70 Mt of pure hydrogen and 20 Mt of hydrogen mixed with other fuel gases for industries like steel manufacturing and methanol production [6]. In recent years, the dynamic performance of H<sub>2</sub> production, particularly focusing on electrolyzers, has garnered

considerable attention in the literature [7, 8]. These studies have emphasised the role of electrolyzers in addressing the intermittency challenge associated with renewable energy sources. Despite these advancements, the current cost of this technology remains a barrier to its seamless integration into the power grid, and other methods like low-carbon natural gas-based hydrogen technology offer the potential to facilitate the widespread adoption of hydrogen technologies for grid stabilisation. Hydrogen is seen as the fuel of the future, with the potential for power generation *via* direct combustion in hydrogen/gas turbines [9]. Mitsubishi Power, Siemens, and General Electric have introduced hydrogen-fuelled gas turbines that use H<sub>2</sub>/CH<sub>4</sub> gas blends [10]. The first purpose-built hydrogen-combustion power plant was opened in 2022 at Long Ridge Energy Terminal in the US, operating at 5% H<sub>2</sub>, with plans to upgrade to 100% hydrogen [11]. More recently, at the UKCCSRC conference in Cardiff, UK (March 28-29, 2023), Richard Little from RWE stated that “*RWE has plans to decarbonise the Pembroke power station via integrating an on-site blue hydrogen production with the natural gas power plant. It is anticipated that the process would result in a ~17% higher reduction in total carbon footprint compared to a natural gas power plant retrofitted with post-combustion carbon capture*”. The recent interest in the incorporation of H<sub>2</sub> into electricity generation from both academia and industry highlights the timely nature of this research and this statement from one of the key industrial players in the country, additionally played a key part in motivating this paper.

Despite hydrogen combustion producing little greenhouse gas emissions, the production of hydrogen from fossil fuels, such as natural gas, resulted in over 900 million metric tons of CO<sub>2</sub> emissions in 2020, accounting for 2.5% of global energy and industrial CO<sub>2</sub> emissions [5]. Many techniques, including water splitting, high-temperature electrolysis (HTE), gasification, wind (or solar) water electrolysis, and steam methane reforming (SMR), can be used to produce hydrogen. However, over 50% of worldwide hydrogen production comes from SMR [12]. In a typical SMR process, methane is converted to H<sub>2</sub> and CO under the reforming reaction (R1) using high-temperature compressed steam. Next, the generated syngas is fed to the shift reactor, where the water-gas shift (WGS) reaction occurs (R2). The use of certain catalysts (i.e., Ni, Fe, Ir, and Pt-based) considerably facilitates both reactions. Since the WGS reaction takes place as a secondary reaction to SMR, the overall reaction can be represented as (R3) [13].



A common practice in SMR involves utilising amine absorption to remove  $\text{CO}_2$  from the reformer's discharge, followed by further refinement of  $\text{H}_2$  to meet commercial hydrogen grades *via* pressure swing adsorption (PSA). However, reaching a high purity of  $\text{H}_2$  is not necessary for mixed-hydrogen-combustion power plants [14].

Thermodynamic constraints and chemical equilibrium limit the SMR and WGS reactions, making it impossible to achieve complete conversion of methane and carbon monoxide in a single reactor. Additionally, the highly endothermic nature of methane reforming (R1) makes the SMR process energy-intensive, resulting in substantial capital and operational costs [15]. Auto-thermal reforming (ATR) and sorption-enhanced steam methane reforming (SE-SMR) are two effective alternatives in the production of *clean* hydrogen.

The ATR process employs the *in-situ* heat generated by the highly exothermic methane combustion reaction (R4) to drive the reactions (R1-R3) [16]. SE-SMR uses *in-situ*  $\text{CO}_2$  sorbents such as  $\text{CaO}$ , to simultaneously remove  $\text{CO}_2$  according to reaction R5. Taking out  $\text{CO}_2$  from the reforming reaction (R3) drives the forward reaction which results in increased hydrogen generation (according to Le-Chatelier's principle) [17]. The combination of these two advancements creates a more compact and intensified process (2-in-1), reducing steam demand and the size of the process while enabling more moderate operating conditions. In addition, at a hydrogen-combustion power plant, on-site hydrogen generation and its immediate use would be a safer option than sourcing hydrogen from an off-site production facility. This approach eliminates the hazards associated with hydrogen transportation and storage [14]. In addition, the minimised transportation and potential storage cost would translate into a more viable process.



Equilibrium models have been mostly adopted to describe SMR reactions and to simulate the reformer. These models have been employed to run sensitivity analyses and to investigate the impact of independent parameters on key performance indicators (KPIs) [18]. This may result in inherent oversimplification of the model, which may lead to some divergence from realistic results. In our work, a rate-based model was employed for the SMR and WGS reactions to simulate the reformer in clean hydrogen production. Using a model based on kinetic data gives a better understanding of the rate at which the reaction proceeds. Moreover, the implementation of a *full factorial design* has allowed us to investigate the presence of any potential interactions among the studied parameters. This leads to a deeper statistical insight into the process and a better understanding of the optimum operating conditions.

This study represents a continuation and derivative of our previous work on a clean hydrogen production process [17], aiming to further explore the implementation of the process for power generation. To the best of our knowledge, there is no

research on investigating hydrogen production *via* SMR coupled with *in-situ* carbon capture and ATR for power generation that has adopted kinetic models and a full-factorial design to investigate the interaction of key parameters on KPIs. As such, herein, our developed clean  $\text{H}_2$  production process is integrated with an on-site hydrogen-combustion power plant where the interaction of key parameters (i.e., temperature, pressure, and steam-to-methane ratio (S/C)) on KPIs (i.e.,  $\text{H}_2$  purity and the generated power) was investigated, followed by the impact of  $\text{H}_2$  purity on the generated power.

## II. METHODOLOGY

### A. Full Factorial Design

Initially, an experimental design table was developed using the *General Full Factorial Design* (GFD) (Design Expert Software v.7) to create a set of experiments (simulation runs) in terms of four independent parameters to investigate their impact and interactions for two KPIs, namely hydrogen purity (mole-%) and power generation (kW). Integration of an ATR unit with the reformer was taken as a *nominal* parameter. The other three parameters are *ordinal*, each with 4 levels: temperature of the feedstock to the reformer (400, 600, 800, and 1000 °C), pressure of the system (1, 10, 20, and 30 bara) and S/C (1, 2.5, 4, and 6 mol/mol).

Accordingly, 128 simulation runs were carried out: 64 runs with ATR, and 64 runs without one. This allowed us to investigate the impact of ATR on hydrogen purity and the generated power. Statistical analysis was used to identify the significant variables and their effects on responses. Subsequently, a model (a basic mathematical model of the simulation) was created to a gain deeper understanding of the impact of variables on KPIs, and to examine any interactions. This is critical as the influence of one variable on KPIs could be linked to the level of another variable. Moreover, the model can predict responses within variable ranges, and identify the optimal variable values for KPI optimisation.

### B. Process Design

Fig. 1 shows the process flow diagram of the hydrogen-combustion power plant with onsite clean hydrogen production. The process modelling was carried out in Aspen Plus (Version 12.1). To describe the SMR and WGS reactions (R1-R3), a kinetic-based model was employed, using the Generalised-Langmuir-Hinshelwood-Hougen-Watson (GLHHW) reaction model. The models were constructed based on the previously published data [19]. Several assumptions were made during the simulation, such as steady-state operation without a temperature gradient in the reactor, ideal gas behaviour, no pressure drop in the process, no degradation in catalyst or sorbent, and no side reactions or adsorption except for those described here.

$\text{CaO}$  carbonation was simulated using a pair of stoichiometric models where the adsorption was implemented in the reformer and the desorption was modelled in a calcination unit. Calcination gives out a  $\text{CO}_2$ -rich stream, which is stored subsequently. The output of the reformer (an  $\text{H}_2$ -rich stream) is fed to the hydrogen-combustion unit.

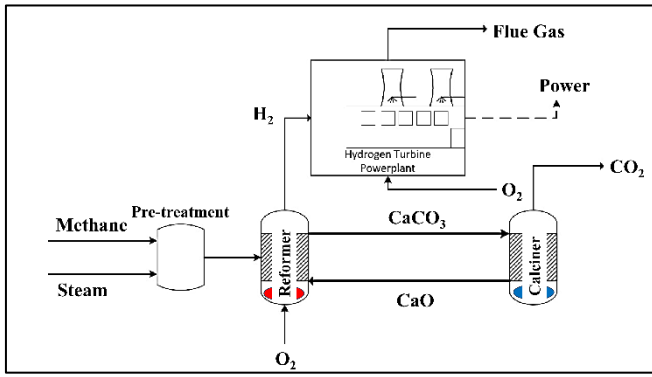


Fig. 1. Process flow sheet for the simulated clean hydrogen production unit with an onsite hydrogen-combustion power plant.

The power generator comprises a combustor and a turbine with the assumption of 65% isentropic efficiency. The H<sub>2</sub>-rich stream from the reformer is mixed with air in the combustor and the outlet is fed into the turbine. The exhaust gas consists of mainly water vapour, CO<sub>2</sub> and hydrogen – depending on the purity of hydrogen in the H<sub>2</sub>-rich stream. Table I summarises the properties of the streams and blocks used in the process.

TABLE I. PROPERTIES OF STREAMS AND BLOCKS

Stream or Block	Properties		
	Components (mole)	Temperature	Pressure
Methane	CH <sub>4</sub> 100% (1000 kmol/hr)	300 °C	1 bara
Steam	H <sub>2</sub> O 100% (1-6 times of Methane)	300 °C	1 bara
Pre-treatment	Compressor and Heater	400-1000 °C	1-30 bara
Reformer	PFR reactor, Requil reactor, Adsorber	Varied	Varied
Calciner	Desorber, Separator	Varied	Varied
O <sub>2</sub>	O <sub>2</sub> 100% (based on the stoichiometry of combustion reaction)	25 °C	1-30 bara
Power	Combustor (Rigibbs reactor), Heater, Turbine	Varied	Varied

### C. Kinetic Model

The rates of reaction (*mol/kg<sub>cat</sub>.s*), based on the Langmuir-Hinshelwood-Hougen-Watson (LHHW) kinetic model, for the reforming reaction (R1), water-gas-shift reaction (R2) and the overall reaction (R3) in the reformer, and with Ni-Al<sub>2</sub>O<sub>3</sub> serving as the catalyst, are expressed according to equations (1-3):

$$R_1 = \frac{k_1}{P_{H_2}^{2.5}} \left( P_{CH_4} P_{H_2O} - \frac{P_{H_2}^3 P_{CO}}{K_I} \right) \left( \frac{1}{\Omega^2} \right) \quad (1)$$

$$R_2 = \frac{k_2}{P_{H_2}} \left( P_{CO} P_{H_2O} - \frac{P_{H_2} P_{CO}}{K_{II}} \right) \left( \frac{1}{\Omega^2} \right) \quad (2)$$

$$R_3 = \frac{k_3}{P_{H_2}^{3.5}} \left( P_{CH_4} P_{H_2O}^2 - \frac{P_{H_2}^4 P_{CO}}{K_{III}} \right) \left( \frac{1}{\Omega^2} \right) \quad (3)$$

In these equations,  $k_{1-3}$  and  $K_{I-III}$  are the reaction rate and equilibrium constants for the (R1-R3), respectively;  $\Omega$  is the adsorption term described as follows:

$$\Omega = 1 + K_{CO} P_{CO} + K_{H_2} P_{H_2} + K_{CH_4} P_{CH_4} + K_{H_2O} \frac{P_{H_2O}}{P_{H_2}} \quad (4)$$

Where,  $K_i$  and  $P_i$  are the adsorption equilibrium constant and the partial pressure of components  $i$ , respectively. The adsorption term uses Van't Hoff parameters, as listed in Table II:

TABLE II. THE VAN 'T HOFF PARAMETERS USED IN THE GENERAL LHHW CORRELATION.

Equilibrium constant	Pre-exponential factor	Unit	E <sub>a</sub> (kJ/mol)
$K_{CH_4}$	6.65E-04	atm <sup>-1</sup>	-38.28
$K_{H_2O}$	1.77E+05	_	-88.68
$K_{H_2}$	6.12E-09	atm <sup>-1</sup>	-82.9
$K_{CO}$	8.23E-05	atm <sup>-1</sup>	-70.65

Aspen Plus, however, does not directly support the rate expression detailed above. Instead, the following equations are the general equations used to describe the LHHW model in Aspen Plus:

$$R = \frac{(\text{kinetic factor}) \times (\text{driving force})}{(\text{adsorption term})} \quad (5)$$

Where,

$$\text{kinetic factor} = k \left( \frac{T}{T_0} \right)^n e^{-\frac{E}{R} \left( \frac{1}{T} - \frac{1}{T_0} \right)} \quad (6)$$

$$\text{driving force} = K_1 \prod_{i=1}^N C_i^\alpha - K_2 \prod_{i=1}^N C_i^\beta \quad (7)$$

$$\text{adsorption term} = \left[ \sum_{i=1}^M K_i \left( \prod_{j=1}^N C_j^M \right) \right]^m \quad (8)$$

$$K = A \exp\left(\frac{B}{T}\right) T^C \exp(DT) \quad (9)$$

Where  $K_i$  is reaction constant,  $C_i$  is concentration,  $T_0$  is reference temperature,  $E$  is activation energy and  $\alpha$ ,  $\beta$ ,  $n$ ,  $N$ ,  $M$ ,  $m$ ,  $A$ ,  $B$ ,  $C$ , and  $D$  are constant parameters and coefficients. Therefore, it was necessary to rearrange equations 1-4 to identify the corresponding model's coefficients and parameters.

In this process, Peng-Robinson thermodynamic fluid package is considered for the entire process. The feed components are steam and methane at atmospheric pressure and 300 °C. The molar flow rate of CaO into the reformer is adjusted based on the mole of CaO in the recycle stream which is produced in the calciner. Except for the reformer, which is described *via* kinetic models, the other reactors are modelled based on equilibrium and stoichiometric assumptions.

## III. RESULTS AND DISCUSSION

The simulation was run according to the full factorial design to investigate how the operational variables interact with the set KPIs.

### A. Effect of Temperature and Pressure

Fig. 2 and 3 demonstrate the impact of temperature and pressure and their interaction on H<sub>2</sub> purity and power generation, respectively, with a constant S/C ratio of 4 as the optimum S/C ratio reported elsewhere [12]. These results pertain specifically to the ATR unit.

Fig. 2 suggests that with an ATR, the temperature of the feed would not significantly affect the final hydrogen purity. This would be, however, not correct for the generated power (Fig. 3). Coupling the ATR with the reformer leads to an increase in the reformer temperature - high enough to produce more hydrogen and CO<sub>2</sub>. Since CO<sub>2</sub> is continuously removed from the reformer, the purity of hydrogen increases. As can be seen, pressure does not affect the purity in the range of temperatures studied. This is different, however, when operating the process under atmospheric pressure conditions. This confirms that with ATR, depending on the hydrogen purity required, one can use a low-temperature feed and medium-to-high pressures.

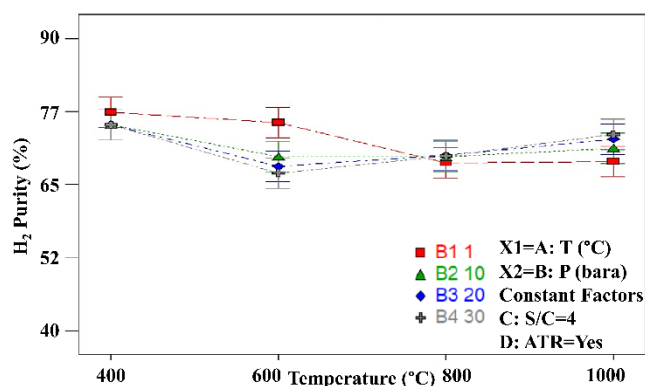


Fig. 2. Effect of temperature and its interaction with pressure on H<sub>2</sub> purity (When S/C= 4 and ATR is utilised).

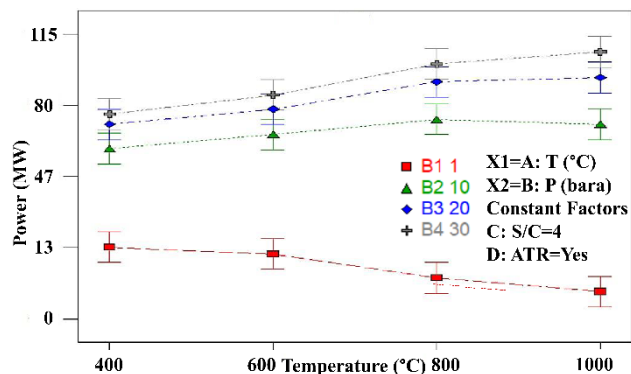


Fig. 3. Effect of temperature and its interaction with pressure on generated power (When S/C= 4 and ATR is utilised).

As we can see in Fig. 3, the higher pressure will help to generate significantly more power regardless of the temperature. However, the trend is exactly the opposite when the process is run at atmospheric pressure. This suggests that the production and utilisation of hydrogen in hydrogen-combustion power plants should be done at > 10 bara; increasing the pressure to 20 bara can increase the generated power by nearly 25%.

### B. Effect of ATR Utilisation

Fig. 4 and 5 show the impact of ATR integration on H<sub>2</sub> purity and power generation at different temperatures. The graphs are produced at the constant S/C ratio of 4 and a pressure of 10 bara.

Fig. 4 confirms our interpretation of the effect of temperature on H<sub>2</sub> purity with ATR integration. The purity of produced hydrogen is not changing significantly within the range of

studied temperatures with the addition of ATR. However, the trend is completely different when no ATR is coupled with the reformer, and the purity of produced hydrogen is directly related to the temperature. In other words, the results indicate that temperature affects the purity of hydrogen; however, using ATR sustains temperatures high enough in the reformer to meet maximum hydrogen purity, regardless of the reformer's feed temperature. This can translate into optimised capital and operating cost due to lower operating temperatures.

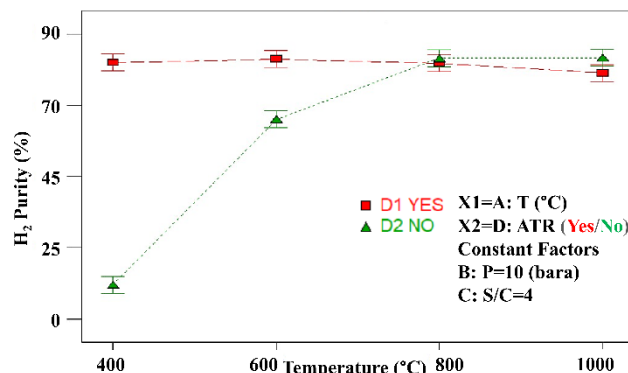


Fig. 4. Effect of ATR integration on hydrogen purity at different temperatures (When S/C= 4 and pressure=10 bara).

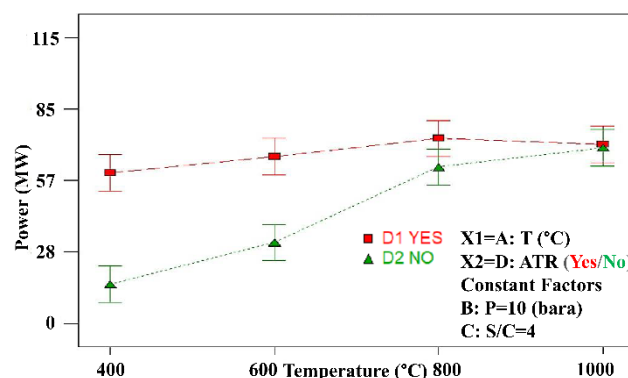


Fig. 5. Effect of ATR integration on generated power at different temperatures (When S/C= 4 and pressure=10 bara).

As for the generated power, with ATR integration, there is some improvement up to 800 °C which is then followed by a slight drop at 1000 °C. This suggests that higher feed temperatures will favour the generated power; however, this should be kept to < 800 °C. In the absence of ATR, temperatures higher than 800 °C can still improve the generated power. This is because, without ATR, heat is to be supplied *via* “pre-treatment” units.

### C. Effect of Steam-to-Methane Ratio

Fig. 6 and 7 illustrate the impact of steam-to-methane (S/C) ratio in different scenarios i.e., with/without ATR, on H<sub>2</sub> purity and power generation, respectively. In these graphs, temperature and pressure are held constant at 800 °C and 30 bara, respectively. This is because it was shown that high temperatures and pressures provide optimal conditions for hydrogen purity and power generation.

Fig. 6 shows the impact of the steam-to-methane ratio on hydrogen purity in two scenarios: with and without ATR. As the

steam-to-methane ratio increases from 1 to 6, hydrogen purity also increases by about 20% in both cases. This behaviour is anticipated since the addition of steam favours the WGS reaction, which produces more hydrogen at the expense of carbon monoxide. The absence of a significant difference between the two scenarios suggests that ATR does not affect hydrogen purity under these conditions. However, it is important to note that this is based on  $T=800\text{ }^{\circ}\text{C}$  and  $P=30\text{ bara}$  which are already favourable for high-purity hydrogen production.

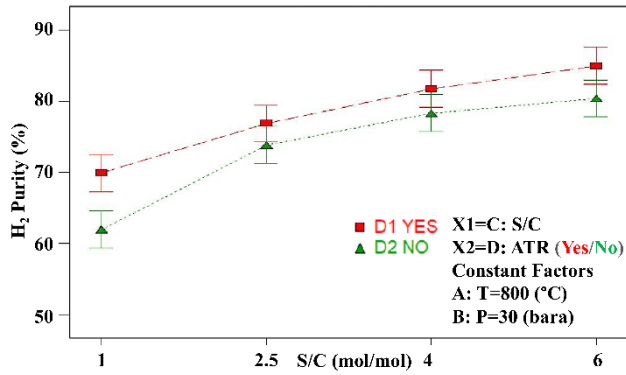


Fig. 6. Effect of steam-to-methane ratio in two scenarios i.e. with/without ATR, on H<sub>2</sub> purity (When Temperature= 800 °C and Pressure=30 bara).

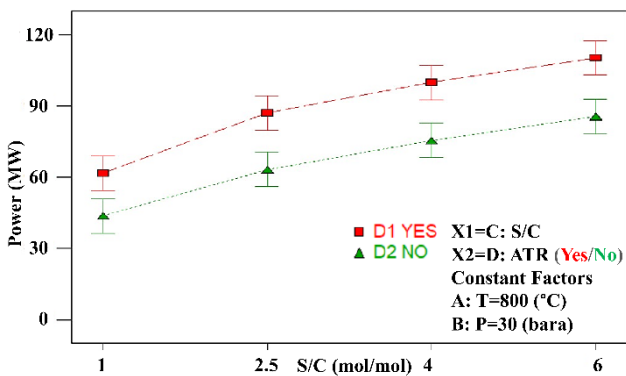


Fig. 7. Effect of steam-to-methane ratio at two scenarios of with/without ATR on generated power (When Temperature= 800 °C and Pressure=30 bara).

Fig. 7 shows the impact of the steam-to-methane ratio on the generated power in the same two scenarios. Again, increasing the steam-to-methane ratio from 1 to 6 results in about a 25% increase in the generated power in both scenarios. However, the graph shows that using ATR leads to much higher power generation compared to the scenario where no ATR is employed. This behaviour is anticipated as ATR provides an additional source of heat that can be used to generate power. The difference between the two scenarios becomes more pronounced as the steam-to-methane ratio increases, indicating that ATR becomes more beneficial as more steam is added. Overall, these graphs provide valuable information on the optimisation of the reforming process for hydrogen production and power generation.

#### D. Effect of Hydrogen Purity on Generated Power

Fig. 8 demonstrates the effect of hydrogen purity on the power output. Here, the entire data for hydrogen purity based on the four independent variables (T, P, S/C, and the ATR) are

collected together with the corresponding generated power for the same independent variables. It can be seen that by increasing the hydrogen purity, the generated power also increases. However, this could be due to other factors such as the temperature and pressure of the reformer's discharge streams. Although high purity of hydrogen in hydrogen-based gas turbines can reduce CO<sub>2</sub> emissions significantly, maintaining such a high level of purity could add to the overall operating costs. On the flip side, impurities such as carbon monoxide and other contaminants can lead to corrosion and fouling of the turbine components and can reduce the efficiency of the power plant.

A blend of hydrogen and natural gas can be a cost-effective option for power generation; however, this depends on various factors such as the availability and cost of natural gas, the design and capacity of the power plant, and the regional environmental regulations.

Fig. 9 depicts a comparison between the with- and without-ATR processes. Optimum purity and power are achieved with ATR integration. Moreover, in both scenarios, the maximum power and hydrogen purity correspond to a pressure of 30 bara and a steam-to-methane ratio of 6. Also, ATR integration can lower the feed temperature to 800 °C, while providing higher hydrogen purity (84.94%), as well as generated power (110 MW).

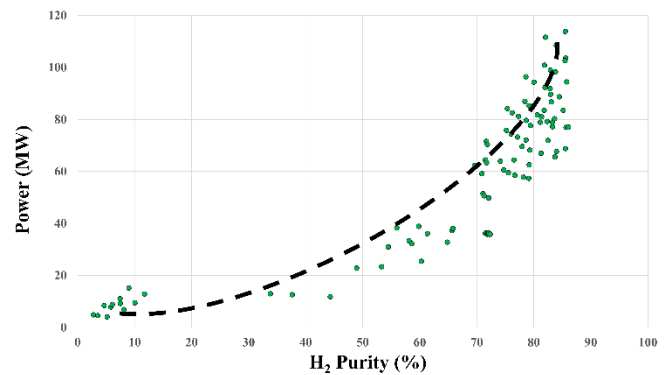


Fig. 8. The correlation between the H<sub>2</sub> purity and the generated power.

## IV. CONCLUSION

This study provided insight into a clean hydrogen production process that was developed by using a kinetic model and integrating it with an onsite hydrogen-combustion power plant. The correlation between the key parameters such as temperature, pressure, and S/C in two scenarios i.e., with and without the integration of an ATR unit, on hydrogen purity and generated power was investigated. Also, the relation between the purity of the produced hydrogen and the generated power was analysed. A full factorial design matrix for simulation runs was employed to investigate the interaction among the operational variables for the prescribed set of KPIs adopted in this work.

The results indicated that the use of ATR led to an increase in the reformer's temperature, which enhanced hydrogen production, and consequently increased hydrogen purity. In other words, the purity of hydrogen was not significantly affected by the feed's temperature with ATR integration, while the opposite was true in the absence of an ATR unit.

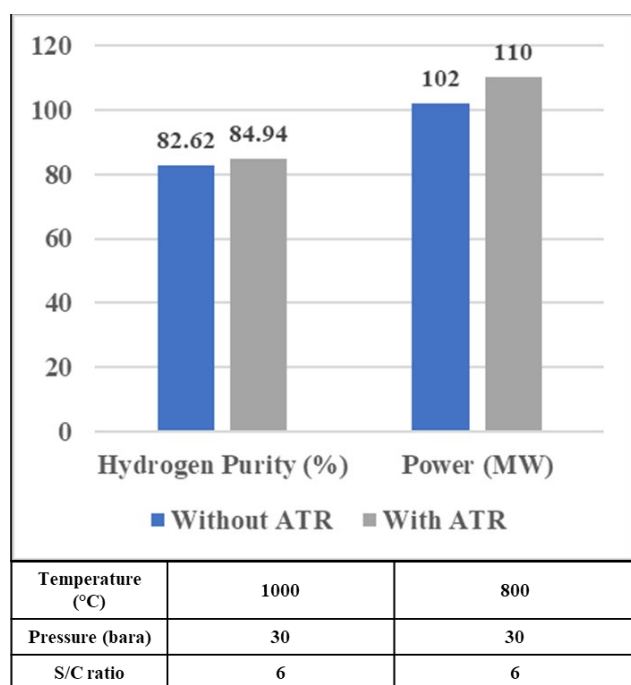


Fig. 9. A comparison between maximum hydrogen purity and generated power with and without ATR integration.

Therefore, capital and operational costs could be optimised due to lower temperatures in the pre-treatment stage. Additionally, it was realised that pressure played a critical role in power generation despite having a relatively less pronounced effect on hydrogen purity in the range of temperatures investigated in this work.

An increase in S/C would result in an increase in hydrogen purity and generated power in both scenarios. However, using ATR led to a much higher power generation compared to the scenario where no ATR was added to the process. Also, the difference between the two scenarios became more significant as the S/C increased, indicating that ATR became more beneficial as more steam was added. Increasing hydrogen purity led to an increase in the generated power. This can help to reduce CO<sub>2</sub> emissions, but it can also increase the associated operating costs. Using a blend of hydrogen and natural gas could be cost-effective, but this would depend on additional factors. Overall, the integration of ATR can be recommended as it could result in higher hydrogen purity and generated power at lower feed temperatures. Further research in this area is of paramount significance.

#### ACKNOWLEDGEMENT

This work has been funded by the UK's Engineering and Physical Sciences Research Council (EPSRC), as part of the UKRI, via the project titled *Multiphysics and multiscale modelling for safe and feasible CO<sub>2</sub> capture and storage* (EP/T033940/1).

#### REFERENCES

- [1] NOAA. National Centers for Environmental Information, State of the Climate: Monthly Global Climate Report for Annual 2021, published online January 2022, retrieved on August 18, 2022
- [2] IPCC, "Climate Change 2022: Mitigation of Climate Change. Contribution of Working Group III to the Sixth Assessment Report of the Intergovernmental Panel on Climate Change," Cambridge University Press, Cambridge, UK and New York, NY, USA, 2022.
- [3] M. Crippa et al., "CO<sub>2</sub> emissions of all world countries - 2022 Report," Publications Office of the European Union, Luxembourg, 2022.
- [4] S. Z. Abbas, V. Dupont, and T. Mahmud, "Modelling of H<sub>2</sub> production in a packed bed reactor via sorption enhanced steam methane reforming process," *Int. J. Hydrogen Energy*, vol. 42, no. 30, pp. 18910-18921, 2017.
- [5] IEA, "Global Hydrogen Review 2021, IEA, Paris," 2021.
- [6] Z. Liu and I. A. Karimi, "Simulating combined cycle gas turbine power plants in Aspen HYSYS," *Energy Convers. Manage.*, vol. 171, pp. 1213-1225, 2018.
- [7] M. B. Hossain, M. R. Islam, K. M. Muttaqi, D. Sutanto, and A. P. Agalgaonkar, "Advancement of fuel cells and electrolyzers technologies and their applications to renewable-rich power grids," *J. Energy Storage*, vol. 62, p. 106842, 2023.
- [8] M. B. Hossain, M. R. Islam, K. M. Muttaqi, D. Sutanto, and A. P. Agalgaonkar, "Power System Dynamic Performance Analysis Based on Frequency Control by Proton Exchange Membrane Electrolyzers," *IEEE Transactions on Industry Applications*, vol. 59, no. 4, pp. 4998-5008, 2023.
- [9] P. A. Pilavachi, S. D. Stephanidis, V. A. Pappas, and N. H. Afgan, "Multi-criteria evaluation of hydrogen and natural gas fuelled power plant technologies," *Appl. Therm. Eng.*, vol. 29, no. 11, pp. 2228-2234, 2009.
- [10] A. Cormos and C. Cormos, "Techno-economic assessment of combined hydrogen & power co-generation with carbon capture: The case of coal gasification," *Appl. Therm. Eng.*, vol. 147, pp. 29-39, 2019.
- [11] A. Schupak, "Hurray For Hydrogen: This New Ohio Power Plant Successfully Used Hydrogen To Generate Electricity.," 2022, April 21.
- [12] S. Masoudi Soltani, A. Lahiri, H. Bahzad, P. Clough, M. Gorbounov, and Y. Yan, "Sorption-enhanced Steam Methane Reforming for Combined CO<sub>2</sub> Capture and Hydrogen Production: A State-of-the-Art Review," *Carbon Capture Science & Technology*, vol. 1, p. 100003, 2021.
- [13] M. M. Shahid, S. Z. Abbas, F. Maqbool, S. Ramirez-Solis, V. Dupont, and T. Mahmud, "Modeling of sorption enhanced steam methane reforming in an adiabatic packed bed reactor using various CO<sub>2</sub> sorbents," *Journal of Environmental Chemical Engineering*, vol. 9, no. 5, p. 105863, 2021.
- [14] Y. Li, H. Yu, X. Jiang, G. Deng, J. Z. Wen, and Z. Tan, "Techno-economic analysis for hydrogen-burning power plant with onsite hydrogen production unit based on methane catalytic decomposition," *Energy Convers. Manage.*, vol. 277, p. 116674, 2023.
- [15] H. H. Faheem, H. U. Tanveer, S. Z. Abbas, and F. Maqbool, "Comparative study of conventional steam-methane-reforming (SMR) and auto-thermal-reforming (ATR) with their hybrid sorption enhanced (SE-SMR & SE-ATR) and environmentally benign process models for the hydrogen production," *Fuel*, vol. 297, p. 120769, 2021.
- [16] G. Ye, D. Xie, W. Qiao, J. R. Grace, and C. J. Lim, "Modeling of fluidized bed membrane reactors for hydrogen production from steam methane reforming with Aspen Plus," *Int. J. Hydrogen Energy*, vol. 34, no. 11, pp. 4755-4762, 2009.
- [17] S. Babamohammadi, W. G. Davies, and S. Masoudi Soltani, "Probing into the interactions among operating variables in blue hydrogen production: A new approach via design of experiments (DoE)," *Gas Science and Engineering*, vol. 117, p. 205071, 2023.
- [18] J. Powell et al., "Optimisation of a sorption-enhanced chemical looping steam methane reforming process," *Chem. Eng. Res. Des.*, vol. 173, pp. 183-192, 2021.
- [19] D. K. Lee, I. H. Baek, and W. L. Yoon, "Modeling and simulation for the methane steam reforming enhanced by in situ CO<sub>2</sub> removal utilizing the CaO carbonation for H<sub>2</sub> production," *Chem. Eng. Sci.*, vol. 59, no. 4, pp. 931-942, 2004.